Available online at www.sciencedirect.com
ScienceDirect
Journal of Magnetic Resonance 192 (2008) 69–77
JMR Journal of Magnetic Resonance
www.elsevier.com/locate/jmr

Sensitive and robust electrophoretic NMR: Instrumentation and experiments

Fredrik Hallberg, István Furó, Pavel V. Yushmanov, Peter Stilbs *

Division of Physical Chemistry and Industrial NMR Centre, Department of Chemistry, Royal Institute of Technology (KTH), Teknikringen 36, Plan 6, SE-10044 Stockholm, Sweden

Received 5 December 2007; revised 1 February 2008
Available online 6 February 2008

Abstract

Although simple as a concept, electrophoretic NMR (eNMR) has so far failed to find wider application. Problems encountered are mainly due to disturbing and partly irreproducible convection-like bulk flow effects from both electro-osmosis and thermal convection. Additionally, bubble formation at the electrodes and rf noise pickup has constrained the typical sample geometry to U-tube-like arrangements with a small filling factor and a low resulting NMR sensitivity. Furthermore, the sign of the electrophoretic mobility cancels out in U-tube geometries. We present here a new electrophoretic sample cell based on a vertically placed conventional NMR sample tube with bubble-suppressing palladium metal as electrode material. A suitable radiofrequency filter design prevents noise pickup by the NMR sample coil from the high-voltage leads which extend into the sensitive sample volume. Hence, the obtained signal-to-noise ratio of this cell is one order of magnitude higher than that of our previous U-tube cells. Permitted by the retention of the sign of the displacement-related signal phase in the new cell design, an experimental approach is described where bulk flow effects by electro-osmosis and/or thermal convection are compensated through parallel monitoring of a reference signal from a non-charged species in the sample. This approach, together with a CPMG-like pulse train scheme provides a superior first-order cancellation of non-electrophoretic bulk flow effects.

Keywords: Electrophoretic NMR; eNMR; Method; Convection; Electro-osmosis; Suppression; Electrophoresis

1. Introduction

Conceived as an idea by Packer [1], experimentally pioneered by Holz et al. [2], and later refined by Johnson et al. [3,4], electrophoretic NMR (eNMR) is an established concept in NMR [5–7]. Potential applications are numerous and include multi-component electrophoretic mobilities of ions and charged entities of *e.g.* polyelectrolytes [8], colloidal particles, biological macromolecules and their counterions in aqueous solution [6,9–13]. Electrostatic considerations are fundamental for the physico-chemical understanding of such systems. eNMR-based studies of battery-related electrolyte systems represent an example of an obvious technical application [14,15].

Despite its clear physico-chemical importance, eNMR does not exists as an option for commercial NMR instrumentation, and to date remains a relatively exotic technique. There are two main underlying reasons. First, the dominantly accepted electrophoretic sample cell design for liquids is based on U-shaped tubes [2] where the bottom part of the U-tube extends into the sensitive sample volume while the electrodes (typically made of blackened platinum metal) enter through the upper tube ends. This arrangement solves three problems, but at a high price. Bubbles that form (by electrolysis) at the electrodes travel upwards and do not induce macroscopic flow. The electrodes themselves are situated outside the sensitive sample volume and therefore noise pickup by the radiofrequency (rf) coil from the electrodes and their connecting cables is reduced. Finally, although the U-tube must be manufactured, the cell can be easily filled and can be readily inserted into

* Corresponding author. Fax: +46 8 7908207.
E-mail address: peter@physchem.kth.se (P. Stilbs).

1090-7807/$ - see front matter © 2008 Elsevier Inc. All rights reserved.
doi:10.1016/j.jmr.2008.02.001

any conventional liquid NMR probe. One immense shortcoming of the U-tube design is its low filling factor which results in a deplorable NMR sensitivity. Even in ^{1}H-detected eNMR, data can seldom be obtained at approximately millimolar concentrations or below. Moreover, the electrophoretic displacements are opposite in the two U-tube halves. Hence, magnetic field gradient-related NMR phase modulation in the tube halves becomes opposite which renders the total signal modulation (assuming that no specialized rf coil arrangements are used) to a cosine function with no sensitivity to the sign of the electrophoretic mobility. Second, several experimental artifacts caused by bulk electro-osmotic and thermal convective flow effects plague eNMR experiments. For quite some years, we have attempted various approaches [16] to provide at least first-order remedies to some of them.

Disturbing bulk-flow effects can be suppressed in various ways. First, a standard chemical procedure to reduce electro-osmotic flow is to coat the sample glass surface with polymer-like materials [17]. Second, one could exploit the observed modulation differences between charged and uncharged species to compensate for bulk flow. This would require access to the sign of displacements by electrophoresis and by bulk flow, however. Third, the wide time-scale separation of build-up of electrophoresis relative to the above mentioned bulk flow effects provide a pathway for separating electrophoresis and electro-osmosis. Basic hydrodynamic considerations yield that a steady-state electrophoretic mobility of an ion or charged entity in aqueous solution appears on a sub-nanosecond time scale upon the application of a DC electric field. Likewise, by reversing the field polarity, an almost instantaneous reversal of the electrophoretic transport will occur. Related bulk phenomena such as electro-osmosis induced by the same electric field and convection as a result of temperature gradients from an uneven Joule heating of the sample develop on much longer time scales of tens of milliseconds or more. Nevertheless, our original attempts some 10 years ago to isolate eNMR-detected electrophoresis from disturbing effects of electro-osmosis were unsuccessful.

In this paper, we present a new sample cell design with several advantages over the conventional U-tube arrangement. As we are going to argue below, it not only offers an order-of-magnitude improvement in NMR sensitivity but, with a new experimental protocol and a new pulse sequence, designed with the above mentioned factors in mind also provides new opportunities for measuring electrophoretic mobilities without systematic errors caused by bulk-flow effects. As an extra bonus, it is straightforward to manufacture and use.

2. Experimental strategies and designs

2.1. Sample cell and rf filters

The disadvantages of the U-tube design were recognized [18–21] early on (among others, by the inventors themselves [19]). Various types of double concentric or straight tube designs have been tested and used over the years [15,18,19,21–25]. Although a cylindrical sample geometry intrinsically provides a high filling factor and preserves the sign of the electrophoretic displacement, there are severe practical shortcomings with designs of this family. One electrode connected from the open top of the probe and the other from the bottom and with cable led through the probe body is a possibility. However, this leads to a cumbersome filling procedure and requires NMR probes adapted to (or built around) the cell. Second, bubbles developing at the bottom electrode move upward and induce macroscopic liquid flow. Although it was stated [18] that alternating electric polarity reduces this problem for platinum black electrodes, from our own experience in the field this reduction seems to be less than sufficient. The double concentric design with both upward and downward current paths does not preserve the sign of the electrophoretic displacement. Morris and Johnson [4,20] proposed an alternative design that consisted of two concentric tubes, the inner one holding the sample and the space between the inner and outer ones a salt solution. These two volumes, each with an electrode inserted from the top, were separated by a conductive gel plug. Although better than a U-tube, the filling factor of this cell is still lower than that in a completely filled NMR tube. The filling procedure is again cumbersome, and the gel plug, while should have no influence on the sample, must also be non-permeable for the molecules in the sample. This may not always be the case.

The sample cell depicted in Fig. 1 consists of a standard thin-wall 5 mm NMR tube with two internal electrodes. The electrode wires are surrounded by an insulating sheath (sealed by glue at the end, which blocks sample liquids to enter the space between the wire and the sheath) except at their respective ends. Here they are wound into flat bundles whose width and shape matches the internal tube diameter. To start with, this arrangement provides us with the highest possible filling factor and with a cell that is both easy to fill and which can be inserted into any NMR probe. To make this cell into a practical eNMR tool, two shortcomings must be eliminated: bubble formation at the bottom electrode and noise pickup from the electrodes by the NMR sample coil. Magnetic field homogeneity limitations with this type of sample cell appeared to be similar to those of a U-tube arrangement—a reasonably symmetric bandshape at decent resolution (<15 Hz at half height) could regularly be achieved.

To suppress bubble formation, we use palladium metal (as 0.5 mm diameter 99.5% wire, from Goodfellow) instead of the traditionally used Platinum for the electrodes. Pd is known to dissociate and absorb hydrogen gas to a considerable extent. Hence, if H_2 is formed at the bottom electrode it is readily removed. Also, a (partially) hydrogen-filled Pd electrode is likely to provide a catalytic re-formation pathway for H_2O near or at the metal surface upon switching the electric field polarity. Although bubble for-

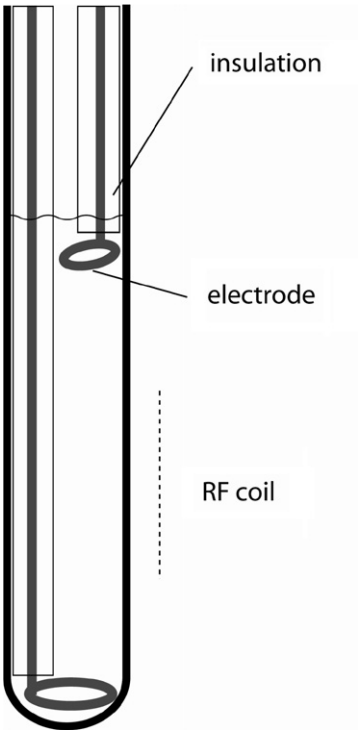

Fig. 1. The electrophoretic sample cell based on a conventional 5 mm NMR tube. The distance between the electrodes was roughly 3 cm. It was found necessary to ensure a snug fit between the electrodes and the glass, to assure mechanical rigidity, since there were otherwise clear signs of (vibration-related) experimental irreproducibility.

mation at Pt-black surfaces is also suppressed to some extent with respect to an untreated Pt surface that effect is probably based on trapping the evolving gases in the porous Pt-black surface layer. Based on visual observation, we find that the current threshold for bubble formation at our Pd electrodes is approximately 40% higher than that at comparable Pt-black electrodes. Indeed, in our setup there was no visually observable bubble formation at all up to approximately 13 mA electrophoretic current.

To prevent noise pickup, a new electronic filter design in the context of eNMR measurements was used throughout. There are two different sources contributing to rf noise at the frequencies and bandwidths of typical NMR experiments: (i) rf interference which is picked up from the surrounding by the long connecting wires between the electrophoretic DC amplifier and the probe working as an antenna, and (ii) rf noise (“noisy ground”) generated predominantly in the digital part (a 500-MHz Pentium II computer and its D/A interface board used for eNMR pulse shape generation) of the electrophoretic signal source. One should note that digital noise cannot simply be suppressed by traditional techniques like single-point grounding and similar [26].

The schematic diagram of our rf interference filter is shown in Fig. 2. The filter consists of two stages, the first one (A) placed in a shielded box inserted halfway between the amplifier and the electrophoretic insert of the NMR probe and the second one (B) placed directly inside this latter insert. The insert is shaped as an NMR sample spinner; the cell in Fig. 1 is plugged into it from below and the connecting leads are fastened to the electrodes inside the insert body. Both A and B constitute standard design schemes for second-order low-pass filters. All capacitors (500 pF, rated for 2 kV maximum voltages) and inductances $\boldsymbol{L}$ (0.1 mH ferrite-cored coil) were scavenged from faulty NMR amplifiers while home-made inductances $\boldsymbol{l}$ (10 μH) contained 100 turns coiled on a 2-mm ceramic tube. Due to the required double polarity of DC currents and the related absence of DC ground in the electrophoretic parts, a double coaxial connecting cable (Twinax $2 * 50\ \Omega$) provided one grounded shield and two ”hot” connections.

Stage A suppresses the “noisy ground” effect [26]; the aluminium body of A has a large capacitance and therefore establishes a “local ground” (in effect, a component with very high capacitance) for the braided shield of the Twinax cable. For safety reasons, the shielding must also be connected to the noisy ground of the electrophoretic power supply via a filtering inductance $\boldsymbol{L}$. Stage B suppresses the RF interference that may come from rest of the coaxial cable. The body of B were made of brass. Hence, the filter components within are shielded and a local ground is established. One should note that this two-stage arrangement was necessary because there is no other reliable high-capacity local ground in and around the electrophoretic insert inside the magnet and because we could not use ferrite-cored inductances at the electrophoretic insert

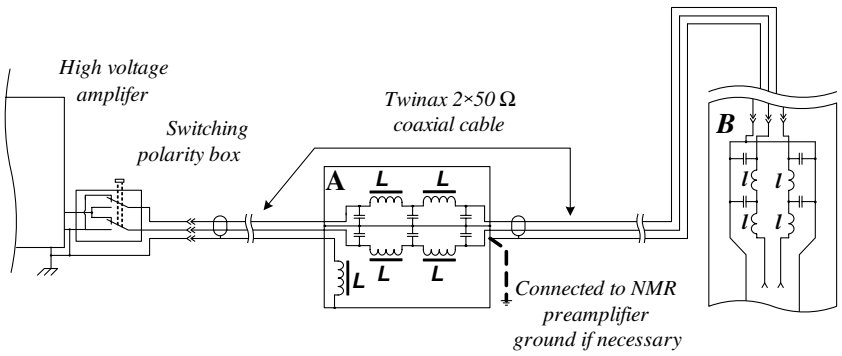

Fig. 2. Schematic picture of the low-pass filter combination for suppressing rf noise in the electrophoretic setup.

since all ferrites are saturated already in >0.1 T magnetic fields.

With the full filter set, we detected roughly the same NMR spectral noise with our connecting cable attached or detached from the electrophoretic insert. Without the filter set, one experienced up to one order of magnitude increase of the NMR spectral noise upon attaching the connecting cable. The signal-to-noise ratio was also significantly worse when only one stage of the full filter set was used.

2.2. CPMG-like eNMR experiments

He and Wei introduced convection compensation in eNMR experiments by using a gradient moment nulling technique [27] as illustrated in Fig. 3. The basic building block is the same as that widely established in various schemes to provide "convection–compensation" to the generic family of PGSE-based self-diffusion experiments [28,29]. Here, it is straightforward to experimentally compensate for thermal convection, because that flow pattern does not depend on the direction of the electrophoretic current. Whether or not the selected procedure suppresses electro-osmosis is more subtle and depends on the time-scale separation between electrophoresis and electro-osmosis. While polarity reversal instantaneously (<ns) reverses electrophoretic drift of molecules or small charged entities; it takes a far longer time (τ_{osm}) for the electro-osmotic flow pattern to develop. This build-up time increases strongly with the tube diameter, with $\tau_{osm} \sim 0.1$ s obtained experimentally [30,31] in non-viscous aqueous solution contained in tubes of a diameter of a few millimeters. Hence, suppression of electro-osmotic displacement would be possible by performing experiments where the polarity is switched faster than τ_{osm}. Then there should be no time for electro-osmosis to develop.

We also found that eNMR experiments based solely on the basic approach [27] suggested by He and Wei (and on its extension to stimulated echo experiments [16]) were not satisfactory in a majority of our past experiments. This might partly be because thermal convection also has a finite build-up time and will likely be stronger during the second of the two electrophoretic pulses. Since the requirement for flow compensation by gradient moment nulling technique [28,29] is constant flow velocity over the duration of 4τ (see Fig. 3), this will predictably lead to less efficient convection compensation.

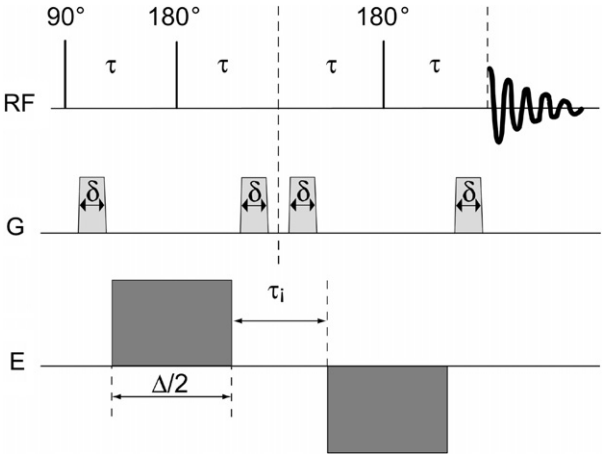

Fig. 3. The eNMR pulse sequence [27] with suppression the effects of thermal convection.

It is straightforward to show that, at the condition of a constant electric field, the volume density of Joule heating is constant upon varying the tube diameter and length. Hence, the temperature gradient in an eNMR experiments depends primarily on the heat flow out of sample volume. On the other hand, convection is easier to induce at larger diameters. For those compounded reasons, the build-up of thermal convection depends on many factors, including probe geometry, the thermal properties of probe and sample, and the timing of current pulses during the complete eNMR experiment. Nevertheless, because of the significantly larger tube diameter used here, we expect thermal convection to be far more prominent than that in the narrow capillaries used for U-tube cells. Recall that the Raleigh number which governs the appearance of thermal convection is a $\sim r^4$ function of tube radius [32–34]. (Also note that the generation of a thermal gradient during the course of an experiment is intrinsic to eNMR. Also, the thermal gradient in eNMR is dominantly radial in contrast to the typically vertical temperature gradients which often arise outside the ambient temperature range in temperature-regulated magnetic field gradient probes [35,36] and plague PGSE-type NMR self-diffusion measurements.)

An obvious remedy to problems presented by the combination of thermal and electro-osmotic convection would be to extend the basic eNMR pulse sequence to a truncated CPMG-like pulse train, like that depicted in Fig. 4. Here, the flow modulation of phase during one electrophoretic displacement period ($\Delta/2n$) is given by

$$\phi = \mu E \frac{\Delta}{2n} \gamma g \delta \tag{1}$$

where μE represents the electrophoretic velocity of the investigated molecular species, n the number of pulse sequence loops, γ the magnetogyric ratio and g the amplitude of the gradient pulse, having a duration δ. By changing the polarity of consecutive electric field pulses, the total phase shift of the acquired FID is accumulated as

$$\phi_{tot} = \mu E \Delta \gamma g \delta \tag{2}$$

while any flow term is cancelled out under the conditions (i) that $\Delta/2n < \tau_{osm}$ and (ii) that τ is sufficiently short for the flow field of thermal convection not to change significantly. One could expect to fulfill these conditions at short echo times.

There are three practical limitations that may determine the area of application of this pulse sequence. First, one must have access to instrumentation, in particular a current

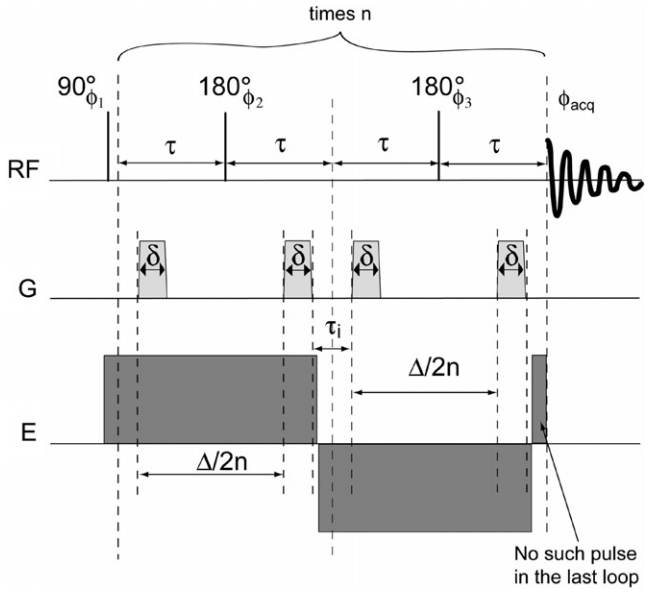

Fig. 4. Schematic sketch of the CPMG-like eNMR pulse sequence. The phase cycle is $\phi_1 = \phi_{acq} = x, -x$; $\phi_2 = \phi_3 = y, -y$.

generator that allows a high rate of polarity switching of the electrophoretic field. Our latest eNMR-instrumental setup uses high-voltage amplifiers with bandwidths exceeding 10 kHz, so polarity switching constraints are no longer a limiting factor in our experiments. Second, a possible complication relative to basic eNMR experiments (which are commonly done with stimulated echoes) is that spin relaxation attenuation during the experiment will become more transverse and less longitudinal. While this is likely a problem for macromolecular or colloidal systems, it should not hamper studies on smaller molecules. Finally and perhaps most seriously, the cumulative effect of electro-osmosis and thermal convection can certainly not be represented as a linear combination of individual flow patterns. Rapid and repeated alternation of electro-osmotic flow direction could even result in chaotic flow patterns.

2.3. Phase detection and phase difference compensation

In our unidirectional sample cell, the signed value of the electrophoretic mobility is extracted from the variation of phase shift (see Eq. (2)) of the signal with increasing electric field in pulse sequences like those in Figs. 3 and 4. This procedure differs radically from that used in U-tube cells where the cosine-like variation of signal intensity with increasing electric field strength provides a measure linked to the magnitude of μ.

We illustrate this difference by investigating the effect of a phase (that is, average velocity during the full experimental time Δ, see Figs. 3 and 4) distribution $\rho(\varphi)$ for uncharged and charged species in an eNMR experiment. The uncharged species may move by electro-osmotic and thermal convection and, since all flow is convective, there is no net material displacement. For some regular stationary flow patterns, such as a parabolic velocity distribution within a tube, the convective part of the phase distribution $\rho_{conv}(\varphi)$ is symmetric. Other velocity profiles as well as acceleration and other non-ideal effects may render $\rho_{conv}(\varphi)$ not symmetric but with a constraint

$$\int_{-\infty}^{0} \varphi \cdot \rho_{conv}(\varphi)\,d\varphi = \int_{0}^{\infty} \varphi \cdot \rho_{conv}(\varphi)\,d\varphi \tag{3}$$

which permits no net flow. Charged species attain an additional unidirectional mobility by electrophoresis and therefore $\rho(\varphi) = \rho_{conv}(\varphi - \varphi_0)$ where φ_0 is the electrophoretic phase factor. The detected intensity of the NMR signal of charged species in a U-tube cell can be obtained from such phase distributions as

$$\begin{aligned} S &\propto \int_{-\infty}^{\infty} \rho_{conv}(\varphi - \varphi_0)\cos(\varphi)\,d\varphi \\ &= \int_{-\infty}^{\infty} \rho_{conv}(\varphi)\cos(\varphi + \varphi_0)\,d\varphi \end{aligned} \tag{4a}$$

which can be re-written as

$$S \propto \cos\varphi_0 \cdot A_c - \sin\varphi_0 \cdot A_s \tag{4b}$$

with

$$A_c = \int_{-\infty}^{\infty} \rho_{conv}(\varphi)\cos\varphi\,d\varphi \tag{4c}$$

$$A_s = \int_{-\infty}^{\infty} \rho_{conv}(\varphi)\sin\varphi\,d\varphi \tag{4d}$$

Since the cosine function is symmetric and flat around zero while the sine function is anti-symmetric, the eNMR signal intensity is dominated by the first term $S \approx \cos\varphi_0 \cdot A_c$. For the same reason, the sensitivity to electrophoretic displacement is rather small and is comparable to the sensitivity to bulk flow. In other words, electrophoretic experiments based on signal intensity detection are hampered unless the electrophoretic displacements are much higher than flow-related ones. In practice, even if the cosine modulation will be dampened by the above mentioned generic bulk flow effects, one can still provide reasonably accurate estimates of φ_0 from the zero crossings of the eNMR signal or through some suitable curve-fitting procedure (on *e.g.* a product of an exponential and a cosine function).

In our unidirectional cell, the complex signal is instead obtained as

$$\begin{aligned} (S_R + iS_I) \propto &\int_{-\infty}^{\infty} \rho_{conv}(\varphi)\cos(\varphi + \varphi_0)\,d\varphi \\ &+ i\int_{-\infty}^{\infty} \rho_{conv}(\varphi)\sin(\varphi + \varphi_0)\,d\varphi \end{aligned} \tag{5}$$

The real part of the signal will be as given in Eq. (4b) and, therefore, the behavior of signal intensity is similar to that obtained in a U-tube. On the other hand, we also attain an imaginary component

$$S_I \propto \cos\varphi_0 \cdot A_s + \sin\varphi_0 \cdot A_c \tag{6}$$

Hence, under the assumption of $A_s = 0$ the phase ϕ of the NMR signal (obtained from $\tan\phi = S_I/S_R$) of our charged species becomes $\phi = \varphi_0$. One should also note that $A_s = 0$ yields zero phase effect for uncharged particles.

Note, however, that Eq. (3) does not exactly predict $A_s = 0$ for a non-symmetrical $\rho_{conv}(\varphi)$ because the sine function is not linear. This effect makes that the phase of the NMR signal deviates from φ_0 and becomes instead given by

$$\tan\phi = \frac{\cos\varphi_0 \cdot A_s + \sin\varphi_0 \cdot A_c}{\cos\varphi_0 \cdot A_c - \sin\varphi_0 \cdot A_s} \tag{7}$$

while the signal of uncharged species ($\varphi_0 = 0$) attains a phase of

$$\tan\phi_u = \frac{A_s}{A_c} \tag{8}$$

From Eqs. (7) and (8) we obtain

$$\tan\phi = \frac{\tan\varphi_0 + \tan\phi_u}{1 - \tan\varphi_0 \cdot \tan\phi_u} = \tan(\varphi_0 + \phi_u) \tag{9}$$

which offers a pathway for compensating for the bulk flow effect. The requirement is to be able to simultaneously monitor the phase shift of neutral monitoring species (as, for other purpose, has been dome by others [37]). Subtracting this from the phase shift observed for charged species, one then arrives at the correct electrophoretic phase information. Note that the same correction procedure also applies for stimulated-echo-type experiments such as EDSTE [16].

While suppression of thermal convection is possible by alternation the electric polarity, that strategy does not work for suppressing electro-osmosis since that flow pattern alters direction in the same way as electrophoresis does. We stress that the phase-difference detection scheme presented above does suppress the effects of both thermal and electro-osmotic flow in an eNMR experiment. In practice, the quality of suppression may also depend on factors like the homogeneity of NMR receptivity over the sample volume.

3. Materials and methods

A solution consisting of 8.6 mM tetramethyl ammonium bromide, TMAB, (analytical grade, Fluka) and 0.0071 mM PEO (analytical grade, Scientific Polymer Products,) with mean molecular weight $M_w = 100{,}000$ g/mol (polydispersity not stated) in D_2O as solvent was used in the experiments performed at 298 K in a Bruker DMX 500 spectrometer. The electrophoretic sample cell based on a standard 5 mm thin-wall NMR tube was inserted into a conventional high-resolution 5 mm NMR probe (Bruker) equipped with a gradient coil of 0.5 T/m maximum gradient at 10 A maximum current. We stress that the tube was used as obtained and was not coated [17] with material that would suppress electro-osmosis.

A Trek PZD700 M/S constant voltage generator was used as electrophoretic voltage amplifier with a maximum voltage and current of ±700 V and 100 mA, respectively. The input pulse shapes to be voltage-amplified by the Trek generator were supplied by a home-made National Instruments LabView program and GUI running on a Pentium-based PC. Compared to previous experiments in U-tube cells [16], the differences between the generators used in the two respective setups reflect differences in sample geometry: the U-tube has a longer current path but a smaller diameter. Since $E = U/l$, where U represents the applied voltage and l the electric field pathway between the electrodes, U-tubes require a higher voltage (but a lower current) to perform experiments at comparable electric field strengths.

The electrophoretic CPMG-like pulse sequence depicted in Fig. 4 was utilized. The total duration of the electrophoretic displacement period (Δ) was set to 500 ms in all experiments and the number of pulse sequence loops (n) were varied between 1, 2, 4 or 8. δ (1 ms) and g (0.26 T/m) were kept constant, and the electrophoretic driving voltage was stepped from 0 to 400 V. The time separation between two consecutive decoding/encoding pulsed field gradients was set to $\tau_i = 2.2$ ms. The polarity of the electric field was reversed and switched 2.0 ms before any encoding gradient pulse. During this time a stable current level would establish itself. The number of time averages was four.

With regard to practical timing constraints of these multi-source CPMG-like pulse sequences we add that eNMR current monitoring was routinely made through a series resistor and a (for safety reasons ground reference floating) battery-operated portable 60 MHz FLUKE 192 Scopemeter, that indicated electrophoretic current switching times of like 1–2 ms. Magnetic field gradient pulses (0.26 T/m) were of standard linear ramped type (five steps during 50 μs).

For comparison, some experiments were also performed by the electrophoretic version of a pulsed field gradient double stimulated echo sequence [16] (EDSTE). All parameters were here set to the same value as for the CPMG-like pulse sequence with $n = 1$.

4. Results and discussion

First and foremost, the NMR signal-to-noise ratio obtained in the new sample cell was approximately one order of magnitude higher than that in a U-tube cell. Further, a substantial improvement in measurement quality was indeed apparent using the suggested CPMG-like eNMR scheme and the equipment described above. When the voltage was stepped up using two electrophoretic pulses ($n = 1$) , bulk flow manifested itself in the form of a signal intensity damping of the uncharged PEO (and HDO) signals, phase shift and distortion of line shapes. All of these bulk flow effects were much reduced in the experiments using the CPMG-like pulse sequence with $n = 2$, 4 and 8 as illustrated for signal damping in Fig. 5.

Fig. 6 illustrates that the phase modulation of the uncharged HDO and the PEO signals differs from that of

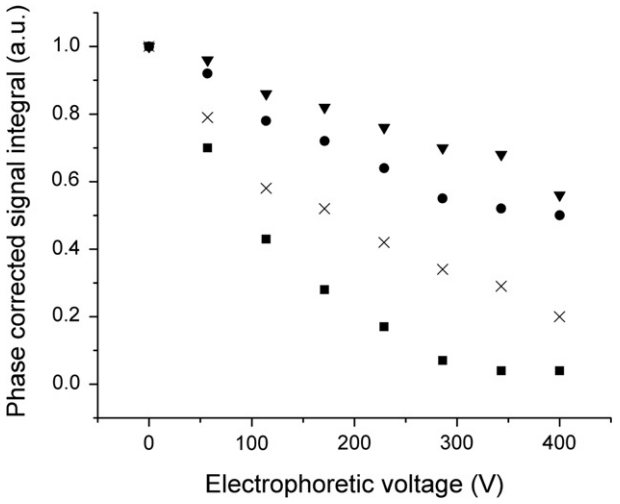

Fig. 5. Normalized signal intensity for uncharged polyethyleneoxide (PEO) molecules recorded upon increasing voltage over our sample cell in Fig. 1 and with experiments with $n = 1$ (■), 2 (×), 4 (●) and 8 (▼) (see Fig. 4).

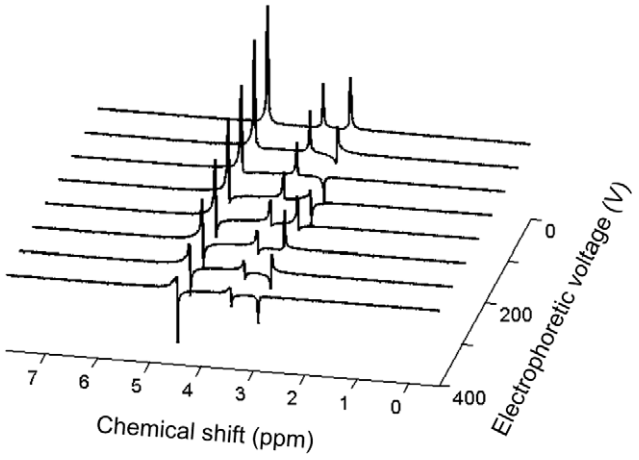

Fig. 6. Stacked plot of spectra from CPMG-type eNMR experiments (with $n = 4$) showing an example of phase modulations of NMR signals at the electrophoretic voltages applied. Signals at 4.5, 3.4 and 2.9 ppm correspond to protons in HDO, PEO and TMA^+, respectively.

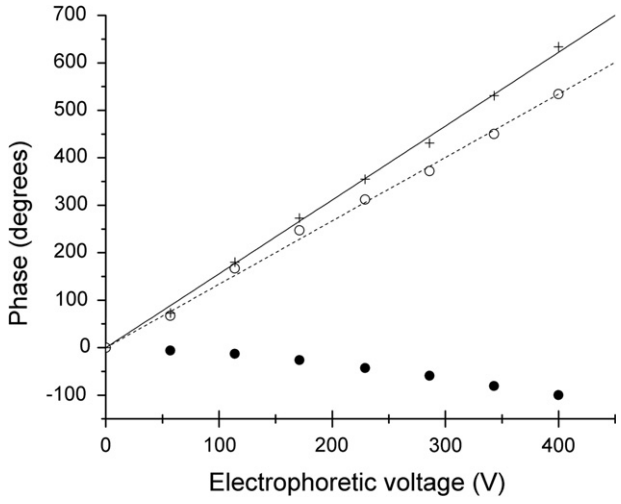

Fig. 7. The phase shifts of the NMR signals of PEO (●) and TMA^+ (○) with increasing electrophoretic voltage in CPMG-type eNMR experiments performed with $n = 4$ (see Fig. 4). The phase difference between TMA^+ and PEO (+) provides the electrophoretic mobility without the effect of electro-osmosis. Linear fits of Eq. 2 to the TMA^+ phases (dashed line) and to the TMA^+/PEO phase differences (solid line) are included.

Table 1
Experimental electrophoretic mobilities of the TMA^+ ion (see also Fig. 8) as obtained in repeated CPMG-type eNMR experiments (see Fig. 4) with and without phase-difference correction (se text)

n	Phase-difference corrected μ ($\times 10^8$ m^2/V s)	μ ($\times 10^8$ m^2/V s)
8	3.86 (±0.03)	4.00 (±0.02)
8	3.90 (±0.02)	3.98 (±0.02)
8	3.92 (±0.02)	4.02 (±0.02)
4	3.76 (±0.02)	3.85 (±0.02)
4	3.76 (±0.02)	3.80 (±0.02)
4	3.76 (±0.02)	3.76 (±0.02)
2	3.75 (±0.04)	3.80 (±0.04)
2	3.71 (±0.03)	3.69 (±0.03)
2	3.70 (±0.04)	3.62 (±0.04)
1	3.79 (±0.04)	4.0 (±0.1)
1	3.83 (±0.06)	3.9 (±0.1)
1	3.79 (±0.05)	4.1 (±0.1)

The error limits in parentheses are 95% confidence intervals as obtained from random scatter of the phase data.

the TMA^+ signal. As discussed above (see Eq. (9)), the experimentally observed difference in the observed phases for two kinds of species in the sample (charged and uncharged) will be used to correct for bulk flow effects. This is illustrated in Fig. 7 where we display the phase shifts of the PEO ($=\phi_u$) and TMA^+ ($=\phi_u - \varphi_0$) signals and their difference as obtained upon increasing voltage over the eNMR sample cell.

By fitting the data as in Fig. 7 to a linear function with zero intercept, we obtain the slope from which one can extract the electrophoretic mobility μ via Eq. (2) and the relation $E = U/l$. The results of repeated experiments are provided in Table 1 and Fig. 8 where, for comparison, we also provide the values as yielded without the flow correction. There are several observations to make. First, the scatter of the obtained mobility values clearly decreased when the bulk flow correction was applied. This points to some irreproducibility of the convectional flow in the cell. Second, mobility data uncorrected for flow and obtained form phase modulation scattered within a range of ±10% for experiments performed with different numbers of CPMG cycles, n. In contrast, the variation of the signal intensity decay with n, displayed in Fig. 5 is much stronger which provides a striking illustration of the inherent robustness of the phase detection method. Third, mobility data corrected for flow effects are all within a range of ±5% but with minimum values obtained at $n = 2$ and 4. Since it is reasonable to expect that motional artifacts primarily increase the apparent electrophoretic mobility, this points to best flow compensation at $n = 2$ and 4. In principle,

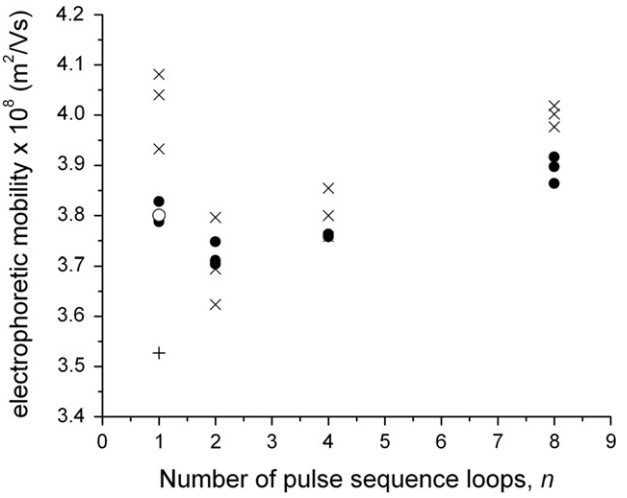

Fig. 8. Experimentally obtained electrophoretic mobilities for the TMA^+ ion: from TMA^+ phases (×) and from TMA^+/PEO phase differences (●) observed in CPMG-type eNMR experiments and from TMA^+ phases (+) and TMA^+/PEO phase differences (○) observed in a double-stimulated-echo eNMR experiment.

one would expect that higher number of CPMG loops would provide better flow compensation. This seems not to be the case for $n > 4$ and we tentatively speculate that the underlying reason could be the evolution of a chaotic, fluctuating flow pattern as a result of repeated electro-osmotic flow reversals with respect to the thermally induced flow. This suggestion is further supported by band-shape distortions observed at $n > 8$. Finally, we note that the scatter of the data obtained with $n = 2$ and 4 is very small, ±1%.

To obtain a quantitatively correct value of μ, one must also know the electrode–electrode distance l. To measure this parameter directly and accurately is not feasible in our cell for two reasons. First, the electrode does not end in a sharp tip (as it customarily does in a U-tube cell) but in an extended bundle of wire. Moreover, in a U-tube made of a capillary, the tube diameter is negligible as compared to the path length of the electric current. Therefore the current (and, hence, the electric field) will by good approximation be parallel to the tube axis. This is not the case in our geometry; the electric field between the electrodes may have a slight orientational and magnitude distribution over the sample volume. Hence, we must calibrate a mean electric field along the direction of the magnetic field gradient. To do this, we rely on the zero concentration electrophoretic mobility value $\mu_0 = 3.79 \times 10^{-8}$ m^2/V s of TMA^+ ions in heavy water as obtained by accurate conductivity measurements [38]. From the experimentally available [39] TMA^+/Br association constant K one can estimate that the TMA^+ mobility in our sample is $\mu = \mu_0(1 + K \cdot c)^{-1}$ where c is the molar concentration. This yields $\mu = 3.76 \times 10^{-8}$ m^2/V s, to which value we set the average electrophoretic mobility obtained in our experiments by $n = 4$ (see Table 1). This calibration procedure which also provides us with an effective electrode–electrode distance $l_{\text{eff}} = 31.6\ (\pm\ 0.1)$ mm. The latter matches well to the visually detectable tip-to-tip distance of 29 mm. Note that this multiplication-by-a-constant calibration does not affect relative proportions of experimental electrophoretic mobilities recorded for multiple components or at multiple experimental conditions (like salinity).

5. Conclusions

The outlined new cell design allows a considerable signal enhancement, solely from the bigger sample volume and the much better filling factor. This clearly extends the experimental range of practically feasible applications of eNMR. However, to avoid a detrimental increase of rf noise introduced into the sample area via the electrodes inside it, we had to add a specially designed rf filter to the electrophoretic voltage leads. We suggest that one may use the same filter design in other possible applications where extended metal objects intrude into the NMR sample space (like *e.g.* in situ temperature calibration or in situ heating).

We also achieved a very good suppression of flow artifacts by combining a flow suppressing pulse sequence with the strategy of signal phase correction using an NMR signal from an uncharged reference component in the same sample. We also show in detail that this phase correction technique is exact, in the limit of constant flow velocities. We stress that this phase-difference detection scheme is unique in a sense that it suppresses the effects of electro-osmosis. To emphasize this point, all experiments presented here were performed without anti-osmotic coating applied on the tube wall.

Work will continue along similar lines. One may perceive that adopting a truly cylindrical sample cell geometry [4,15,18–25,40,41] without any lead through the rf-coil-sensitive volume would lead a potential further improvement. Indeed, a change in that direction would eliminate the need for rf filters but would, at the same time, render eNMR less available since then it should be performed in custom-built probes. In the present approach the sample holder would have to be custom built, but this is a trivial task in comparison. Our present design fits into conventional NMR probes and uses conventional NMR tubes without any additional modification, which may facilitate a wider spread of this powerful technique, eNMR.

Acknowledgments

We thank Professor Paul T. Callaghan for suggesting renewed efforts with CPMG-like eNMR sequences. Professor Göran Lindbergh is thanked for useful discussions and advice concerning the electrochemical properties of palladium. We thank the Swedish Research Council (VR) and the Knut and Alice Wallenberg Foundation for financial support.

References

[1] K.J. Packer, The study of slow coherent molecular motion by pulsed field magnetic resonance, Mol. Phys. 17 (1969) 355.

[2] M. Holz, M. Lucas, O. Müller, NMR in the presence of an electric current. Simultaneous measurements of ionic mobilities, transference numbers, and self-diffusion coefficients using an NMR pulsed-gradient experiment, J. Magn. Reson. 58 (1984) 294–305.

[3] T.R. Saarinen, C.S. Johnson, High-resolution electrophoretic NMR, J. Am. Chem. Soc. 110 (1988) 3332–3333.

[4] K.F. Morris, C.S. Johnson, Mobility-ordered two-dimensional nuclear magnetic resonance spectroscopy, J. Am. Chem. Soc. 114 (1992) 776–777.

[5] M. Holz, Electrophoretic NMR, Chem. Soc. Rev. 35 (1994) 165–174.

[6] C.S. Johnson, Electrophoretic NMR, in: D.M. Grant, R.K. Harris (Eds.), Encyclopedia of Nuclear Magnetic Resonance, Wiley, New York, 1996, pp. 1886–1895.

[7] P.C. Griffiths, A. Paul, N. Hirst, Electrophoretic NMR studies of polymer and surfactant systems, Chem. Soc. Rev. 35 (2006) 134–145.

[8] U. Böhme, U. Scheler, Counterion mobility and effective charge of polyelectrolytes in solution, Macromol. Symp. 211 (2004) 87–92.

[9] Q. He, Y. Liu, H. Sun, E. Li, Capillary array electrophoretic NMR of proteins in biological buffer solutions, J. Magn. Reson. 141 (1999) 355–359.

[10] U. Böhme, U. Scheler, Effective charge of bovine serum albumin determined by electrophoresis NMR, Chem. Phys. Lett. 435 (2007) 342.

[11] P.C. Griffiths, A. Paul, P. Stilbs, E. Petterson, Electrophoretic nuclear magnetic resonance (EMR)—a new tool for studying counterion binding in mixed surfactant systems, Langmuir 19 (2003) 8605–8607.

[12] P.C. Griffiths, E. Petterson, P. Stilbs, A.Y.F. Cheung, A.M. Howe, A.R. Pitt, Electrophoretic nuclear magnetic resonance studies of mixed anionic–nonionic surfactant micelles, Langmuir 17 (2001) 7178–7181.

[13] E. Pettersson, D. Topgaard, P. Stilbs, O. Söderman, Surfactant/nonionic polymer interaction: a NMR diffusometry and NMR electrophoretic investigation, Langmuir 20 (2004) 1138–1143.

[14] M. Ise, K.D. Kreuer, J. Maier, Electroosmotic drag in polymer electrolyte membranes: an electrophoretic NMR study, Solid State Ionics 125 (1999) 213.

[15] K. Hayamizu, S. Seki, H. Miyashiro, Y. Kobayashi, Direct in situ observation of dynamic transport for electrolyte components by NMR combined with electrochemical measurements, J. Phys. Chem. B 110 (2006) 22302–22305.

[16] E. Pettersson, I. Furó, P. Stilbs, On experimental aspects of electrophoretic NMR, Concepts Magn. Reson. A 22A (2004) 61–68.

[17] S. Hjérten, High-performance electrophoresis elimination of electroendosmosis and solute adsorption, J. Chromatogr. A 347 (1985) 191–198.

[18] F.M. Coveney, J.H. Strange, E.G. Smith, The measurement of the electrophoretic mobility in surfactant systems using NMR, Mol. Phys. 75 (1992) 127–137.

[19] M. Holz, D. Seiferling, X.A. Mao, Design of a new electrophoretic NMR probe and its application to $^{7}Li^{+}$ and $^{133}Cs^{+}$ mobility studies, J. Magn. Reson. A 105 (1993) 90–94.

[20] K.F. Morris, C.S. Johnson, Mobility-ordered 2D NMR spectroscopy for the analysis of ionic mixtures, J. Magn. Reson. 100 (1993) 67–73.

[21] F.M. Coveney, J.H. Strange, A.L. Smith, E.G. Smith, NMR studies of electrophoretic mobility in surfactant systems, Colloids Surf. 36 (1989) 193–198.

[22] H. Dai, S. Sanderson, J. Davey, F. Uribe, T.A. Zawodzinski, Electrophoretic NMR measurements of lithium transference numbers in polymer gel electrolytes, Proc. Electrochem. Soc. 96 (1997) 111–120.

[23] H. Dai, T.A. Zawodzinski, Determination of lithium ion transference numbers by electrophoretic nuclear magnetic resonance, J. Electrochem. Soc. 143 (1996) L107–L109.

[24] T.A. Zawodzinski, H. Dai, S. Sanderson, J. Davey, F. Uribe, A rapid method for the determination of lithium transference numbers, Proc. Electrochem. Soc. 96 (1997) 103–110.

[25] M. Holz, Field-assisted diffusion studied by electrophoretic NMR, in: P. Heitjans, J. Kärger (Eds.), Diffusion in Condensed Matter, Springer, Berlin, 2005, pp. 717–742.

[26] H.W. Ott, Noise Reduction Techniques in Electronic Systems, Wiley, New York, 1988.

[27] Q. He, Z. Wei, Convection compensated electrophoretic NMR, J. Magn. Reson. 150 (2001) 126.

[28] A. Jerschow, N. Müller, Suppression of convection artifacts in stimulated-echo diffusion experiments. Double-stimulated-echo experiments, J. Magn. Reson. 125 (1997) 372–375.

[29] P.T. Callaghan, Principles of Nuclear Magnetic Resonance Microscopy, Clarendon Press, Oxford, 1991.

[30] B. Manz, P. Stilbs, B. Jönsson, O. Söderman, P.T. Callaghan, NMR imaging of the time evolution of electroosmotic flow in a capillary, J. Phys. Chem. 99 (1995) 11297–11301.

[31] M. Minor, A.J. van der Linde, H.P. van Leeuwen, J. Lyklema, Dynamic aspects of electrophoresis and electroosmosis: a new fast method for measuring particle mobilities, J. Colloid Interf. Sci. 189 (1997) 370–375.

[32] A. Bejan, Convection Heat Transfer, Wiley, New York, 1995.

[33] G.S. Charlson, R.L. Sani, Thermoconvective instability in abounded cylindrical fluid layer, Int. J. Heat Mass Transfer 13 (1970) 1479–1496.

[34] G.S. Charlson, R.L. Sani, On thermoconvective instability in a bounded cylindrical fluid layer, Int. J. Heat Mass Transfer 14 (1971) 2157–2160.

[35] H. Hedin, I. Furó, Temperature imaging by ^{1}H NMR and suppression of convection in NMR probes, J. Magn. Reson. 131 (1998) 126–130.

[36] N. Hedin, T.Y. Yu, I. Furó, Growth of C12E8 micelles with increasing temperature. A convection-compensated PGSE NMR study, Langmuir 16 (2000) 7548–7550.

[37] S.R. Heil, M. Holz, A mobility filter for the detection and identification of charged species in complex liquid mixtures by ENMR phase difference spectroscopy, Angew. Chem., Int. Ed. 35 (1996) 1717–1720.

[38] R.L. Kay, D.F. Evans, The conductance of the tetraalkylammonium halides in deuterium oxide solutions at 25 °C, J. Phys. Chem. 69 (1965) 4216–4221.

[39] J. Mbuna, T. Takayanagi, M. Oshima, S. Motomizu, An investigation of weak ion association equilibria between inorganic anions and tetraalkylammonium ions in ethanol-aqueous media using capillary zone electrophoresis, Bull. Chem. Soc. Jpn. 77 (2004) 1465–1475.

[40] M. Holz, S. Heil, I. Schwab, Electrophoretic NMR studies of electrical transport in fluid-filled porous systems, Magn. Reson. Imag. 19 (2001) 457–463.

[41] S. Wong, U. Scheler, Electrophoresis of macromolecules in solution detected by electrophoresis–NMR, Colloid Surf. A 195 (2001) 253–257.